

## PART V: STARS – II



## Section 13

# Nuclear reactions in stars

### 13.1 Introduction

In general, nuclear processes in stars involve fission of a nucleus, or (more usually in ‘normal’ evolutionary phases), the fusion of two nuclei. Through all these processes, key physical quantities are conserved:

- the baryon number (the number of protons, neutrons, and their antiparticles);
- the lepton number (electrons, neutrinos, related light particles, and their antiparticles);
- charge; and
- total mass–energy.

Consider two types of nuclei,  $A$  and  $B$ , number densities  $n(A)$ ,  $n(B)$ . The rate at which a particular (nuclear) reaction occurs between particles moving with relative velocity  $v$  is

$$r(v) = n(A) n(B) v \sigma(v) \tag{13.1}$$

(per unit volume per unit time) where  $\sigma(v)$  is the cross-section for the reaction. Of course, we need to integrate over velocity to get the total reaction rate:

$$\begin{aligned} r &= n(A) n(B) \int v \sigma(v) f(v) dv \\ &\equiv n(A) n(B) \langle \sigma(v) v \rangle \quad [ \text{m}^{-3} \text{s}^{-1} ] \end{aligned} \tag{13.2}$$

where  $f(v)$  is the (Maxwellian) velocity distribution, and the angle brackets denote a weighted average (i.e., the integral in the first part of eqtn. 13.2).

Since the reaction destroys  $A$  (and  $B$ ), we have

$$\frac{\partial n(A)}{\partial t} = -n(A) n(B) \langle \sigma(v) v \rangle; \quad (13.3)$$

and the number density of species  $A$  falls with time as

$$n(A, t) = n_0(A) \exp \{-n(B) \langle \sigma(v) v \rangle t\} \quad (13.4)$$

which defines a characteristic ( $e$ -folding) timescale

$$\tau = \frac{1}{n(B) \langle \sigma(v) v \rangle}. \quad (13.5)$$

Finally, the total energy generated through this reaction, per unit mass per unit time, is

$$\begin{aligned} \varepsilon &= \frac{Q r}{\rho} \\ &= \frac{n(A) n(B)}{\rho} Q \langle \sigma(v) v \rangle \quad [\text{J kg}^{-1} \text{ s}^{-1}] \end{aligned} \quad (13.6)$$

where  $Q$  is the energy produced per reaction and  $\rho$  is the mass density.

## 13.2 Tunnelling

Charged nuclei experience Coulomb repulsion at intermediate separations, and nuclear attraction at small separations. In stellar cores the high temperatures give rise to high velocities, and increased probability of overcoming the Coulomb barrier. For nuclear charge  $Z$  (the atomic number), the energy needed to overcome the Coulomb barrier is

$$E_C \simeq \frac{Z_1 Z_2 e^2}{r_0} \quad (13.7)$$

$$(\simeq 2 \times 10^{-13} \text{ J}, \quad \simeq 1 \text{ MeV, for } Z_1 = Z_2 = 1) \quad (13.8)$$

where  $r_0 \simeq 10^{-15} \text{ m}$  is the radius at which nuclear attraction overcomes Coulomb repulsion for proton pairs.

In the solar core,  $T_c \sim 1.5 \times 10^7 \text{ K}$ ; that is,  $E (= 3/2 kT) \simeq \text{keV}$ , or  $\sim 10^{-3} E_C$ . This energy is only sufficient to bring protons to within  $\sim 10^3 r_0$  of each other; this is much too small to be effective, so reactions only occur through a process of “quantum tunneling” (barrier penetration). In this temperature regime the rate of nuclear energy generation is well approximated by a power-law dependence on temperature,

$$\varepsilon \simeq \varepsilon_0 \rho T^\alpha \quad (13.9)$$

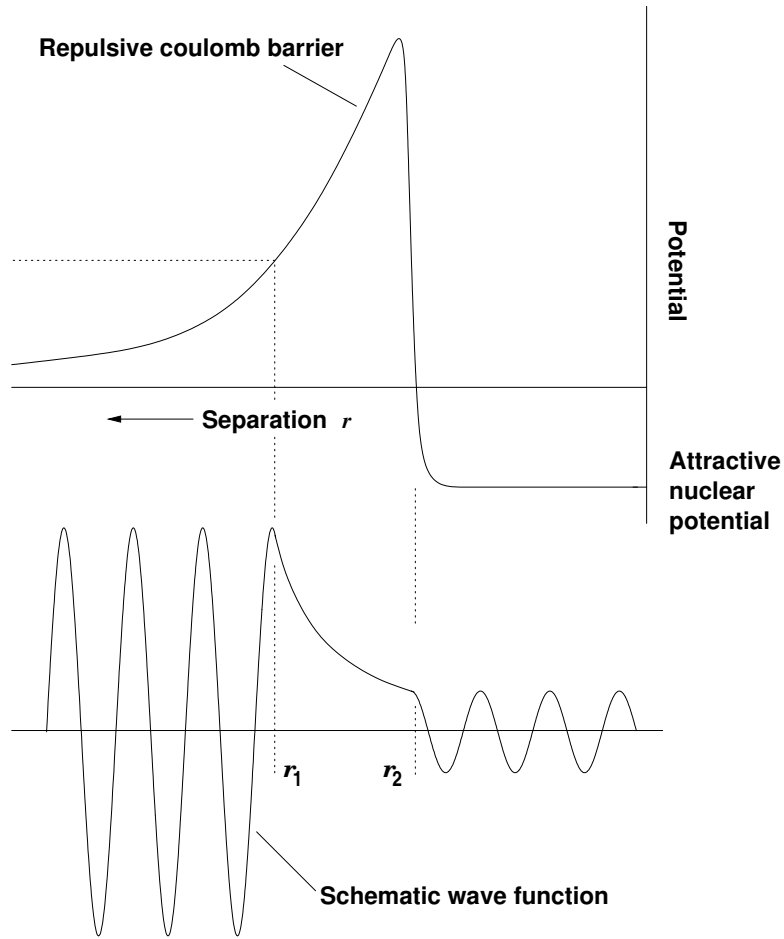


Figure 13.1: Upper section: a schematic plot of the potential between two charged nucleons as a function of separation. At ‘large’ separations ( $\gtrsim 10^{-15}$  m), the repulsive Coulomb force is given by eqtn. (13.8); classically, particles cannot come closer than the point  $r_1$  at which the relative kinetic energy corresponds to the repulsive potential. Quantum-mechanical tunneling allows the nucleons to approach closer, to separation  $r_2$ , at which point the strong nuclear force dominates.

The lower panel expresses this tunnelling schematically. The (square of the) amplitude of the wave function is a measure of the probability of a particle being in a particular location; the amplitude of the wave function decreases exponentially between  $r_1$  and  $r_2$ , but does not fall to zero. (See Aside 13.1 for further details.)

where  $\alpha \simeq 4.5$  for proton-proton reactions in the Sun [Section 13.4;  $\varepsilon_0 \propto n^2(\text{H})$ ], and  $\alpha \simeq 18$  for CN processing [Section 13.5;  $\varepsilon_0 \propto n(\text{H})n(\text{C}, \text{N})$ ].

[Note that eqtn. (13.9) characterizes the rate of energy generation per unit *mass* (or, if you like, per nucleon). Although density appears here as a simple linear multiplier, reference to eqtn. 13.6 reminds us that, like nearly all ‘collisional’ processes, the energy generation rate per unit *volume* – or the probability of a given nucleus undergoing fusion – depends on density *squared*.]

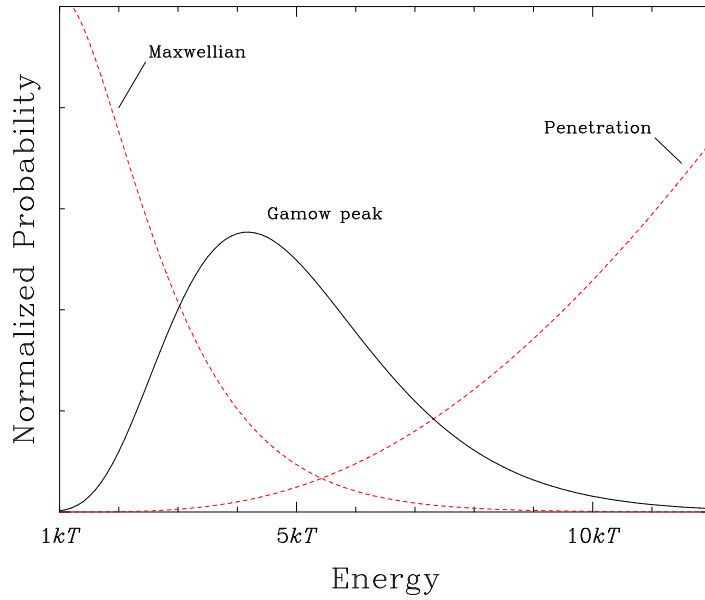


Figure 13.2: The main energy-dependent factors determining two-body reaction rates are the numbers of reagents as a function of energy (the Maxwellian velocity distribution) and the tunnelling probability of penetration. The product of these two terms gives the energy distribution of particles participating in fusion. These factors are illustrated here, on arbitrary vertical scales, for the fusion of two protons in the solar core (Gamow energy  $E_G = 290kT$  for  $T = 2 \times 10^7$  K;  $E_0 = 4.2kT$ ,  $1/e$  width  $\Delta = 4.8kT$ ). See Aside 13.1.

### Aside 13.1: The Gamow Peak

As illustrated in Fig. 13.1, ‘tunnelling’ can occur to allow fusion to occur at particle energies which classical mechanics would indicate to be too low to overcome the Coulomb barrier. For higher temperatures (and larger kinetic energies), particles will come closer together ( $r_1$  approaches  $r_2$ ), the decay of the wave function is reduced, and so the amplitude of the wave function in the region  $r < r_2$  becomes larger – that is, the tunnelling probability increases as the kinetic energy of the incoming nucleus increases.

Obtaining the probability of barrier penetration,  $p_p$ , for given energy, is a standard problem in wave mechanics. We simply quote the result that the probability of penetration varies exponentially with the ratio of kinetic energy to barrier size,

$$p_p \propto \exp \left\{ - \left( \frac{E_G}{E} \right)^{1/2} \right\} \quad (\text{A-13.1})$$

with the ‘Gamow energy’  $E_G$  (unnamed and written as  $b^2$  in some sources) given by

$$E_G = 2m_R c^2 (\pi\alpha Z_1 Z_2)^2 \quad (= 493 \text{ keV for proton-proton fusion}), \quad (\text{A-13.2})$$

where  $\alpha$  is the fine structure constant,

$$\alpha = \frac{e^2}{4\pi\epsilon_0\hbar c} \simeq \frac{1}{137}. \quad (\text{A-13.3})$$

and  $m_R$  is the ‘reduced mass’,

$$m_R = \frac{m_1 m_2}{m_1 + m_2}$$

for particles of mass  $m_1, m_2$  ( $\simeq A_1 m(\text{H}), A_2 m(\text{H})$ ) of charge  $Z_1, Z_2$ . (Using the reduced mass means that velocities and kinetic energies are measured with reference to the centre of mass of the particles involved.)

The fusion cross-section  $\sigma(v)$  (eqn 13.1) is evidently dependent on this penetration probability. We also expect it to depend on the effective size, or ‘target area’, of the particles; this geometrical factor is proportional to  $\pi\lambda^2$ , where  $\lambda$  is the de Broglie wavelength,  $\lambda^2 \propto 1/E$ . The intrinsic properties of the nuclei must also be involved; these will be constant, or slowly varying functions of energy, in most circumstances (although resonances may occur). We therefore write the total reaction cross-section in the form

$$\sigma(E) = \frac{S(E)}{E} \exp \left\{ - \left( \frac{E_G}{E} \right)^{1/2} \right\} \quad (\text{A-13.4})$$

where  $S(E)$  encapsulates the nuclear physics of the actual fusion process.

At any given temperature, the number of particles in a Maxwellian velocity distribution falls off exponentially with increasing energy (eqn. 8.15); that is, the probability of encountering a particle with energy  $E$  at kinetic temperature  $T$  is

$$f(E) dE = \frac{2}{\sqrt{\pi}} \frac{E}{kT} \exp \left\{ - \frac{E}{kT} \right\} \frac{dE}{(kTE)^{1/2}} \quad (\text{A-13.5})$$

These two competing factors – the increasing probability of penetration with increasing energy (eqn. A-13.1) and the decreasing number of particles with increasing energy (eqn. A-13.5) – mean that there is a limited range of energies at which most reactions occur. This is illustrated in Fig. 13.2; the product of the two exponential terms leads to the ‘Gamow peak’, where the probability of fusion occurring is at a maximum.<sup>1</sup>

To explore this in greater detail, we write the reaction rate per particle pair, eqn. 13.2, as

$$\langle \sigma(v) v \rangle = \int_0^\infty \sigma(E) v f(E) dE$$

where  $\sigma(E), v$  are particle cross-sections and velocities at energy  $E$ ; from eqtns. (A-13.4) and (A-13.5), and using  $E = \frac{1}{2} m_R v^2$ ,

$$\langle \sigma(v) v \rangle = \int_0^\infty \frac{S(E)}{E} \exp \left\{ - \left( \frac{E_G}{E} \right)^{1/2} \right\} \sqrt{\frac{2E}{m_R}} \frac{2}{\sqrt{\pi}} \frac{E}{kT} \exp \left\{ - \frac{E}{kT} \right\} \frac{dE}{(kTE)^{1/2}} \quad (\text{A-13.6})$$

$$= \left( \frac{8}{\pi m_R} \right)^{1/2} \frac{1}{(kT)^{3/2}} \int_0^\infty S(E) \exp \left\{ - \frac{E}{kT} - \left( \frac{E_G}{E} \right)^{1/2} \right\} dE \quad (\text{A-13.7})$$

at some fixed temperature  $T$ . Eqtn. (A-13.7) is the integral over the Gamow peak; the larger the area, the greater the reaction rate.

The Gamow peak is appropriately named in that it is indeed quite strongly peaked; it is therefore a reasonable approximation to take the  $S(E)$  term as locally constant. In that case, the integrand peaks at energy  $E_0$ , when

$$\frac{d}{dE} \left\{ \frac{E}{kT} + \left( \frac{E_G}{E} \right)^{1/2} \right\} = \frac{1}{kT} - \frac{1}{2} \left( \frac{E_G}{E_0^3} \right)^{1/2} = 0;$$

i.e.,

$$E_0 = \left( \frac{kT\sqrt{E_G}}{2} \right)^{2/3} \quad (\text{A-13.8})$$

$$= \left[ \sqrt{2} (\pi \alpha k c)^2 m_R (Z_1 Z_2 T)^2 \right]^{1/3}$$

---

<sup>1</sup>Clearly, the area under the Gamow peak determines the total reaction rate.

$E_0$ , the location of the Gamow peak, is the most effective energy for thermonuclear reactions; it greatly exceeds  $kT$ , the typical thermal energy, but falls well below the Gamow energy of the Coulomb barrier.

There is no simple analytical solution for the width of the peak, but one common (and reasonable) approach is to approximate the exponential term in the integral (eqtn. A-13.7) with a gaussian centred on  $E_0$ . Conventionally, in this context 'the' width is not characterized by the gaussian ' $\sigma$ ' parameter, but rather by  $\Delta$ , the full width at  $1/e$  of the peak value (so  $\Delta \equiv 2\sqrt{2}\sigma$ ); thus we need to solve for

$$\exp\left\{-\frac{E}{kT} - \left(\frac{E_G}{E}\right)^{1/2}\right\} \simeq C \exp\left\{-\left(\frac{E - E_0}{\Delta/2}\right)^2\right\}. \quad (\text{A-13.9})$$

Requiring the two sides to be equal at  $E = E_0$  we immediately find

$$\begin{aligned} C &= \exp\left\{-\frac{E_0}{kT} - \left(\frac{E_G}{E_0}\right)\right\}, \\ &= \exp\left\{-\frac{3E_0}{kT}\right\} \end{aligned} \quad (\text{from eqtn. A-13.8})$$

while requiring the curvatures (second derivatives) on either side of eqtn. A-13.9 to be equal gives, after some algebra,

$$\Delta = \sqrt{\frac{16}{3}E_0kT}.$$

The total reaction rate depends on the integrated area under the Gamow peak; again using a gaussian approximation to the peak, and constant  $S(E)$  across the peak, then from eqtn. (A-13.7), we have

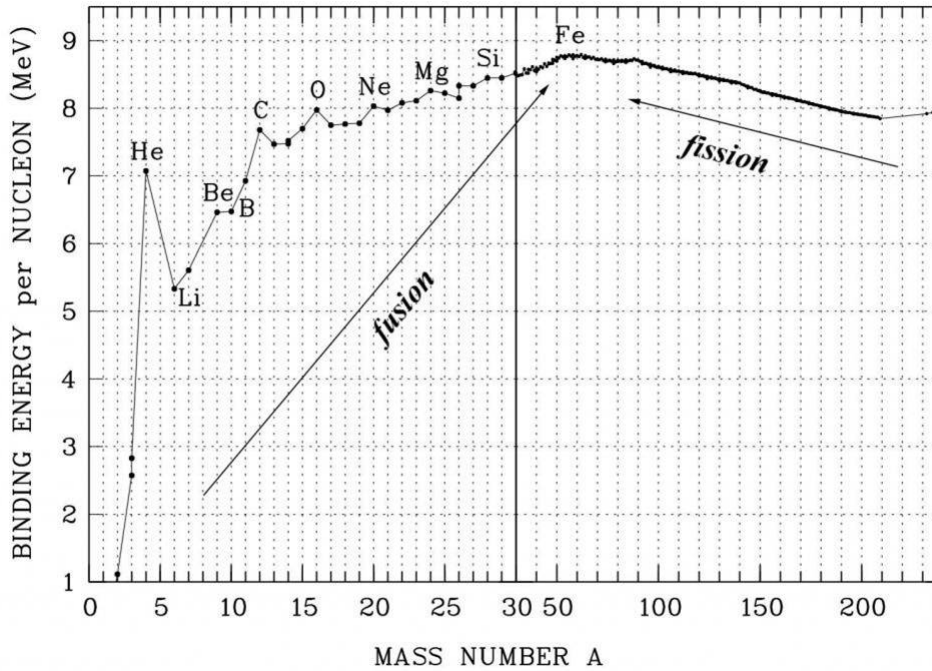
$$\begin{aligned} \langle \sigma(v)v \rangle &= \left(\frac{8}{\pi m_R}\right)^{1/2} \frac{S(E_0)}{(kT)^{3/2}} \exp\left\{-\frac{3E_0}{kT}\right\} \int_0^\infty \exp\left\{-\left(\frac{E - E_0}{\Delta/2}\right)^2\right\} dE, \\ &\simeq \left(\frac{8}{\pi m_R}\right)^{1/2} \frac{S(E_0)}{(kT)^{3/2}} \exp\left\{-\frac{3E_0}{kT}\right\} \frac{\Delta\sqrt{\pi}}{2} \end{aligned} \quad (\text{A-13.10})$$

(where, in order to perform the integration analytically, the limits have been extended from  $0/+ \infty$  to  $-\infty/+ \infty$ ; the error thus introduced is negligible provided that  $E_0 > \Delta/2$ ). Bowers & Deeming give a mathematical development from this point which leads to a demonstration that  $\varepsilon \simeq \varepsilon_0 \rho T^\alpha$  (eqtn. 13.9).

Furthermore, substituting eqtn. (A-13.8) into eqtn. (A-13.7) we obtain

$$\langle \sigma v \rangle \propto \exp[-(E_G/kT)^{1/3}].$$

### 13.3 The mass defect and nuclear binding energy



The mass of any nucleus is less than the sum of the separate masses of its protons and neutrons. The *binding energy* of a particular isotope is the energy corresponding to the ‘missing’ mass (or *mass defect*), and is the energy produced in forming that isotope from its raw ingredients; equivalently, it is the amount of energy needed to break it up into protons and neutrons.<sup>2</sup> The binding energy peaks in the iron group, with <sup>62</sup>Ni the most tightly-bound nucleus, followed by <sup>58</sup>Fe and <sup>56</sup>Fe;<sup>3</sup> this is the basic reason why iron and nickel are very common metals in planetary cores, since they are produced as end products in supernovae.

For atomic masses  $A \gtrsim 60$ , energy release is through *fission* (generally involving much less energy).

For a nucleus with  $Z$  protons,  $N (= A - Z)$  neutrons, and mass  $m(Z, N)$  the binding energy is therefore

$$Q(Z, N) = [Zm_p + Nm_n - m(Z, N)] c^2 \quad (13.10)$$

<sup>2</sup>The binding energy explains why the masses of the proton and neutron are both larger than the ‘atomic mass unit’, or amu; the amu is defined to be  $1/12$  the mass of <sup>12</sup>C, but each nucleon in that isotope has given up almost 1% of its mass in binding energy.

<sup>3</sup>Many sources cite <sup>56</sup>Fe as the most tightly bound nucleus; see M.P. Fewell, Am.J.Phys., 63, 653, 1995 for a discussion which lays the blame for this misconception squarely at the door of astrophysicists!

(where  $m_p$ ,  $m_n$  are the proton, neutron masses), and the binding energy per baryon is

$$Q(Z, N)/(Z + N).$$

Converting ‘MeV per baryon’ to ‘J kg<sup>-1</sup>’, we find that burning protons into helium yields

$$\text{H} \rightarrow \text{He}: \quad 6.3 \times 10^{14} \text{ J kg}^{-1}$$

but

$$\text{H} \rightarrow \text{Fe}: \quad 7.6 \times 10^{14} \text{ J kg}^{-1};$$

that is, burning H to He alone releases 83% of the total nuclear energy available per nucleon.

## Physical processes

To do –

Nuclear models (liquid-drop, shell)

Line of stability (neutron, proton drip lines)

## 13.4 Hydrogen burning – I: the proton–proton (PP) chain

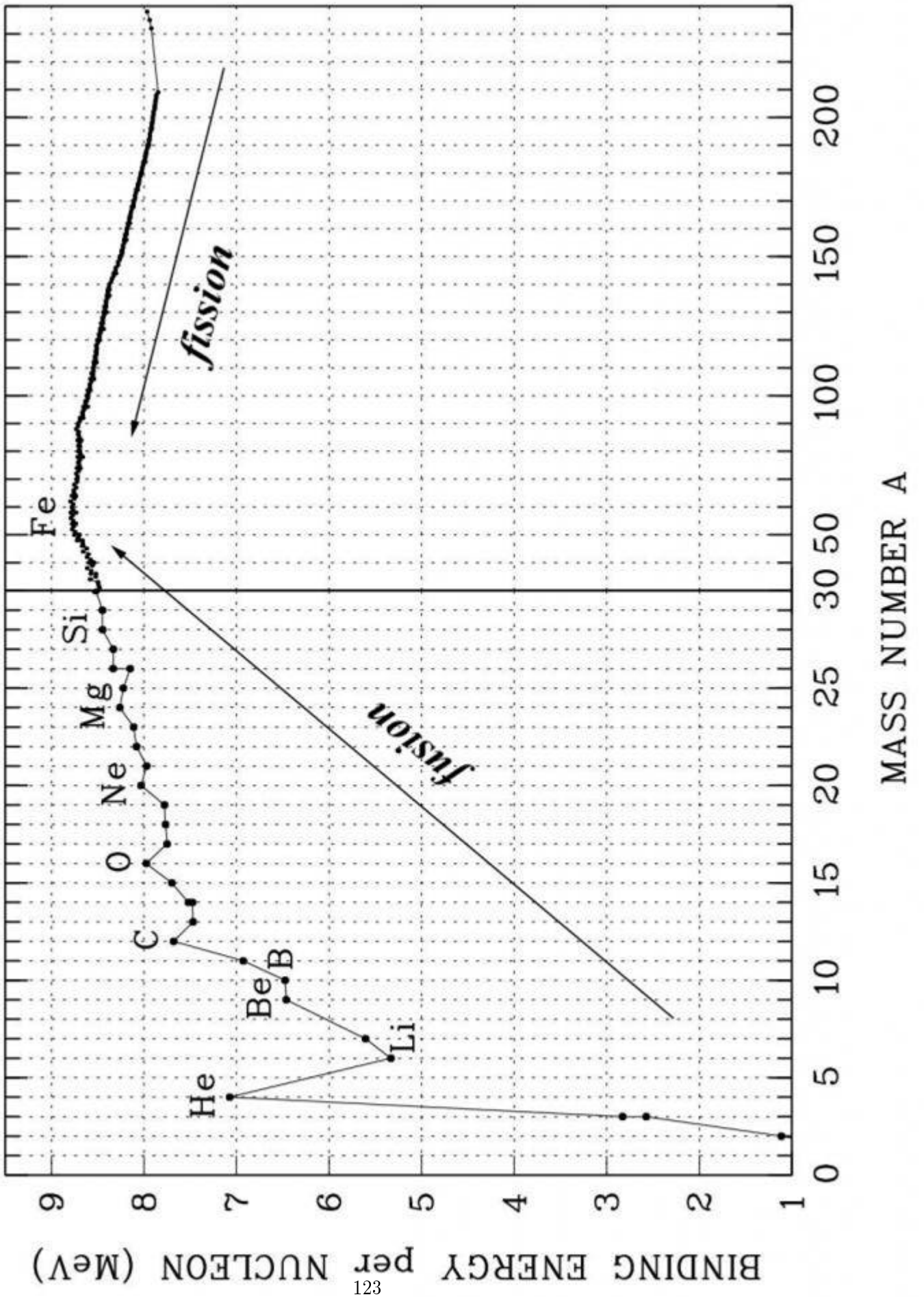
### 13.4.1 PP–I

Step	Process	Energy Release	Solar Timescale
(1)	$p + p \rightarrow {}^2\text{D} + e^+ + \nu_e$	1.44 MeV †	$7.9 \times 10^9$ yr
(2)	${}^2\text{D} + p \rightarrow {}^3\text{He}$	5.49 MeV	1.4s
		<u>6.92 MeV</u> ×2	
(3a)	${}^3\text{He} + {}^3\text{He} \rightarrow {}^4\text{He} + p + p$	12.86 MeV	$2.4 \times 10^5$ yr
		<u>26.72 MeV</u>	

†Includes 1.02 MeV from  $e^+ + e^- \rightarrow 2\gamma$

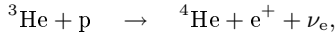
Reaction (1) is very slow because it involves the *weak interaction*,<sup>4</sup> which is required to operate during the short period when protons are close together.

<sup>4</sup>i.e., involves  $\beta$  decay; in this case  $\beta^+$  decay,  $p^+ \rightarrow n^0 + e^+ + \nu_e$  (cp.  $\beta^-$  decay,  $n^0 \rightarrow p^+ + e^- + \bar{\nu}_e$ ).



Reactions (2) and (3a) involve the *strong interaction* and in consequence are much faster.

[Note that reaction (3a) is preferred to



even though protons vastly outnumber  ${}^3\text{He}$  particles, because this again involves the weak interaction (the  $\nu_e$  is the giveaway).]

Reaction (1) occurs twice for each  ${}^4\text{He}$  production, each time generating an electron neutrino with energy 0.26 MeV. These leave the Sun without further interaction, so the energy available for heating is 26.2 MeV ( $26.72 - 2 \times 0.26$  MeV).

### 13.4.2 PP–II, PP–III

There are two principal secondary channels in the proton-proton chain, each catalysed by a pre-existing  $\alpha$  particle ( ${}^4\text{He}$  nucleus):

PP–II (follows steps 1 & 2, which yield 6.92 MeV):

Step	Process	Energy Release	Solar Timescale
(1)	$\text{p} + \text{p} \rightarrow {}^2\text{D} + \text{e}^+ + \nu_e$	1.44 MeV †	$7.9 \times 10^9$ yr
(2)	${}^2\text{D} + \text{p} \rightarrow {}^3\text{He}$	5.49 MeV	1.4s
(3b)	${}^3\text{He} + {}^4\text{He} \rightarrow {}^7\text{Be}$	1.59 MeV	$9.2 \times 10^5$ yr
(4b)	${}^7\text{Be} + \text{e}^- \rightarrow {}^7\text{Li} + \nu_e$	0.86 MeV	0.39 yr
(5b)	${}^7\text{Li} + \text{p} \rightarrow {}^4\text{He} + {}^4\text{He}$	<u>17.35 MeV</u>	570s
		<u>26.72 MeV</u>	

†Includes 1.02 MeV from  $\text{e}^+ + \text{e}^- \rightarrow 2\gamma$

In this case, neutrino losses average 0.80 MeV.

PP–III (follows steps 1, 2, and 3b):

Step	Process	Energy Release	Solar Timescale
(1)	$\text{p} + \text{p} \rightarrow {}^2\text{D} + \text{e}^+ + \nu_e$	1.44 MeV †	$7.9 \times 10^9$ yr
(2)	${}^2\text{D} + \text{p} \rightarrow {}^3\text{He}$	5.49 MeV	1.4s
(3b)	${}^3\text{He} + {}^4\text{He} \rightarrow {}^7\text{Be}$	1.59 MeV	$9.2 \times 10^5$ yr
(4c)	${}^7\text{Be} + \text{p} \rightarrow {}^8\text{B}$	0.14 MeV	66 yr
(5c)	${}^8\text{B} \rightarrow {}^8\text{Be}^* + \text{e}^+ + \nu_e$	16.04 MeV †	1 s
(6c)	${}^8\text{Be}^* \rightarrow {}^4\text{He} + {}^4\text{He}$	<u>3.30 MeV</u>	$10^{-16}$ s
		<u>26.72 MeV</u>	

†Includes 1.02 MeV from  $\text{e}^+ + \text{e}^- \rightarrow 2\gamma$

Neutrino losses here are 7.2 MeV on average, predominantly through step (5c).<sup>5</sup>

In the Sun, ~91% of reactions go through (3a); ~9% end at (5b); and ~0.1% end at (6c).

## 13.5 Hydrogen burning – II: the CNO cycle

Because the first reaction in the PP chain is so slow ( $7.9 \times 10^9$  yr), under certain circumstances it is possible for reactions involving (much less abundant) heavier nuclei, acting as catalysts, to proceed faster than PP. The larger charges (and masses) of these heavier particles imply that higher temperatures are required. Of these processes, the CNO, or CNO-I, cycle<sup>6</sup> is the most important:

Step	Process	Energy Release	Solar Timescale
(1)	${}^{12}_6\text{C} + \text{p} \rightarrow {}^{13}_7\text{N}$	1.94 MeV	$1.3 \times 10^7$ yr
(2)	${}^{13}_7\text{N} \rightarrow {}^{13}_6\text{C} + \text{e}^+ + \nu_e$	2.22 MeV †	7 m
(3)	${}^{13}_6\text{C} + \text{p} \rightarrow {}^{14}_7\text{N}$	7.55 MeV	$2.7 \times 10^6$ yr
(4)	${}^{14}_7\text{N} + \text{p} \rightarrow {}^{15}_8\text{O}$	7.29 MeV	$3.2 \times 10^8$ yr
(5)	${}^{15}_8\text{O} \rightarrow {}^{15}_7\text{N} + \text{e}^+ + \nu_e$	2.76 MeV †	82 s
(6a)	${}^{15}_7\text{N} + \text{p} \rightarrow {}^{12}_6\text{C} + {}^4_2\text{He}$	4.96 MeV	$1.1 \times 10^5$ yr
		<u>26.72 MeV</u>	

†Includes 1.02 MeV from  $\text{e}^+ + \text{e}^- \rightarrow 2\gamma$

As in PP, we have created one  ${}^4\text{He}$  from four protons, with release of some 26.7 MeV in the process; the neutrinos carry off 1.71 MeV for every  $\alpha$  particle created, so 25 MeV is available to heat the gas. Although steps (2) and (5) both involve the weak interaction, they proceed faster than reaction (1) of the PP chain, since the nucleons involved are already bound to each other (which allows more time for the weak interaction to occur).

<sup>5</sup>It is the high-energy neutrinos from this reaction that were famously searched for by experimentalist Raymond Davis and his partner theoretician John Bahcall; the failure to detect them in the expected numbers became known as the ‘Solar Neutrino Problem’. The ‘problem’ is now resolved through better understanding of neutrino physics – the electron neutrinos (the only type of neutrino detectable in the 1960s, ’70s, and ’80s) ‘oscillate’ to other neutrino flavours.

<sup>6</sup>Sometimes called the ‘carbon cycle’, although this risks confusion with cycling of carbon between the Earth’s atmosphere, biosphere, hydrosphere, which also goes by that name. The CNO-I and CNO-II cycles together constitute the ‘CNO bi-cycle’. Where do the CNO nuclei come from? The answer is that they were created in previous generations of stars, in processes shortly to be described.

The cycle starts *and finishes* with  $^{12}\text{C}$ , which acts as a catalyst.<sup>7</sup> However, during CNO cycling, the overall abundances nonetheless change – why is this?

Step (4),  $^{14}\text{N} + \text{p}$ , is more than  $10\times$  slower than the next-slowest reaction (step (1),  $^{12}\text{C} + \text{p}$ ). It therefore acts as a ‘bottleneck’, with a build-up of  $^{14}\text{N}$  at the expense of  $^{12}\text{C}$  until the reaction rates<sup>8</sup> of steps (1) and (4) are equal (these depending on the number densities of reagents; eqn. (13.2)). The equilibrium condition that reaction rates are equal determines the abundances, which can be compared to ‘solar’ abundances:

	CN cycle	Solar	
$n(^{12}\text{C})/n(^{13}\text{C})$	4	89	
$n(^{14}\text{N})/n(^{15}\text{N})$	2800	250	[ $^{15}\text{N}$ reduced by step (6a)]
$n(^{14}\text{N} + ^{15}\text{N})/n(^{12}\text{C} + ^{13}\text{C})$	21	0.3	[ $^{14}\text{N}$ increased by step (3)]

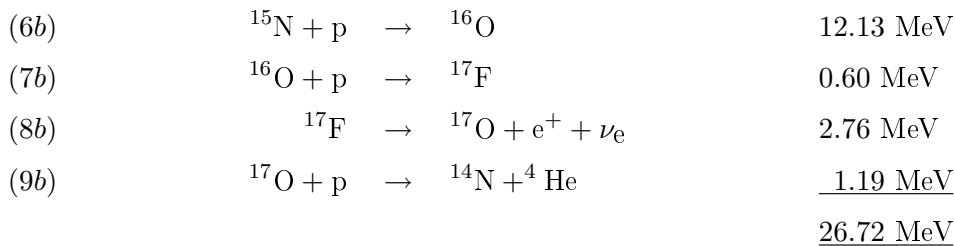
at  $T \sim 1.3 \times 10^7 \text{K}$  (the solar-core temperature; the timescale required to establish equilibrium is set by the slowest reaction, and so is  $\sim 10^8$  yr at this temperature). These anomalous abundance patterns are a clear signature of CN processing if the products are brought to the stellar surface.

We can similarly evaluate equilibrium abundances for PP processing; for  $T \simeq 1.3 \times 10^7 \text{K}$ ,

$$\begin{aligned} n(^2\text{D})/n(^1\text{H}) &= 3 \times 10^{-17} \\ n(^3\text{He})/n(^1\text{H}) &= 10^{-4} \\ & (= 10^{-2} \text{ at } 8 \times 10^6 \text{K}) \end{aligned}$$

### 13.5.1 CNO-II

There are a number of subsidiary reactions to the main CNO cycle, particularly involving oxygen. The CNO-II bi-cycle accounts for about 1 in 2500  $^4\text{He}$  productions in the Sun:



which returns to step (4) in CNO-I

---

<sup>7</sup>Note that given ordering is arbitrary – the cycle can be considered as beginning at any point [e.g., starting at step (4), ending at (3)].

<sup>8</sup>Recall that reaction rates depend on both timescales and reagent abundances – cf. eqn13.1

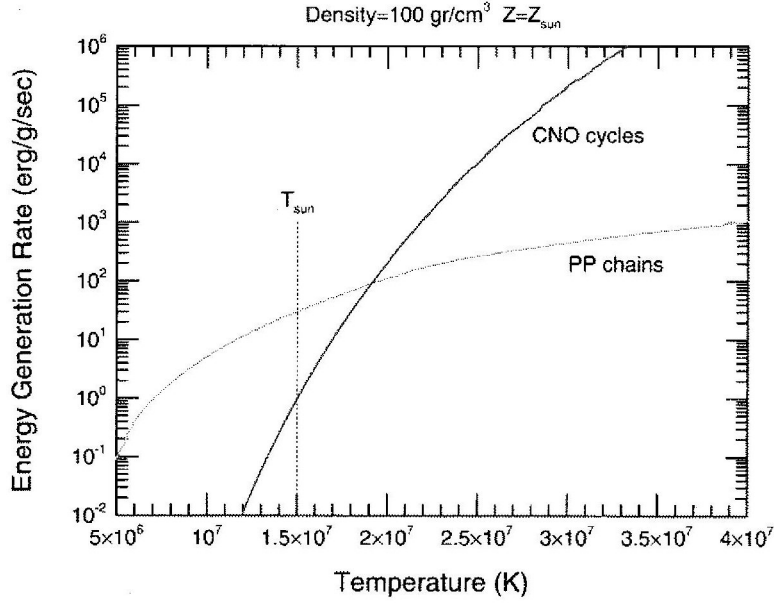
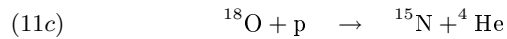
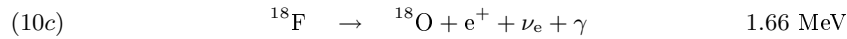
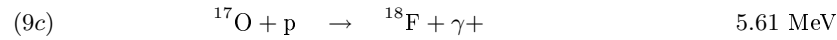


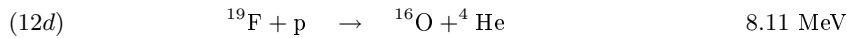
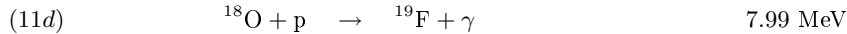
Figure 13.3: Energy generation rates: CNO vs. PP processing

### CNO-III, IV

The ‘OF cycle’ (which with CNO-I and CNO-II makes up the ‘CNO tri-cycle’) occurs in massive stars, and can be divided into CNO-III and CNO-IV; each branch starts from a  $^{17}\text{O}$  produced in CNO-II:

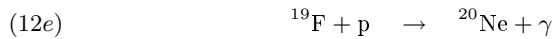


which returns to step (6b) in CNO-II; or, proceeding to CNO-IV:



which returns to step (7b) in CNO-II

The only possible breakout from a closed cycle at temperatures relevant for quiescent hydrogen burning would be an alternative to step (12d),



but the rate is negligibly small, ensuring that the CNO cycles are completely closed.

We have seen that

$$\varepsilon \simeq \varepsilon_0 \rho T^\alpha \tag{13.9}$$

where  $\alpha \simeq 4.5$  for proton-proton reactions in the Sun and  $\alpha \simeq 18$  for CN processing. Because core temperature scales with mass (Section 10.6.3), PP dominates for lower-mass stars, while CN cycling dominates for higher-mass stars. The Sun lies just below the crossover point (fig. 13.5.1), and although the PP chain dominates, the CN cycle is not negligible.

## 13.6 Helium burning

### 13.6.1 $3\alpha$ burning

Hydrogen burning dominates the stellar lifetime (the main-sequence phase), but the core pressure,

$$P = \frac{\rho k T}{\mu m(\text{H})},$$

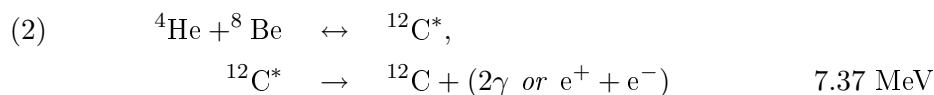
reduces as the mean molecular weight  $\mu$  changes from 0.5 (for fully-ionized pure hydrogen) to 4/3 (for fully-ionized pure helium). As a consequence the core contracts, and heats. If the star is more massive than about  $0.5M_\odot$  the resulting core temperature and pressure are high enough to ignite helium burning ( $\sim 10^8\text{K}$ ,  $10^8 \text{ kg m}^{-3}$ ; lower-mass stars don't have enough gravitational potential energy); the reactions have a nett effect of



However, the process is hindered by the absence of stable mass-5 ( ${}^4\text{He} + \text{p}$ ) and mass-8 ( ${}^4\text{He} + {}^4\text{He}$ ) nuclei; in particular, the  ${}^8\text{Be}$  is unstable, and decays back to a pair of alpha particles in only about  $10^{-16}\text{s}$ . Nonetheless, in equilibrium a small population of  ${}^8\text{Be}$  particles exists (at a level of 1 for every  $\sim 10^9$   $\alpha$  particles) and these can interact with  ${}^4\text{He}$  under stellar-core conditions. Exceptionally, because the lifetimes are so short, the production of  ${}^{12}\text{C}$  is, essentially, a *3-body* process, with an energy-generation rate:

$$\varepsilon_{3\alpha} \simeq \varepsilon_0 \rho^2 T^{30}$$

(where  $\varepsilon_0 \propto n({}^4\text{He})$  and the density-*squared* dependence is because of the three-body nature of the reaction).

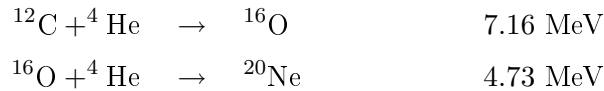


The first stage is endothermic;  ${}^8\text{Be}$  is more massive than two  ${}^4\text{He}$  nuclei, so the relative binding energy is *negative*.

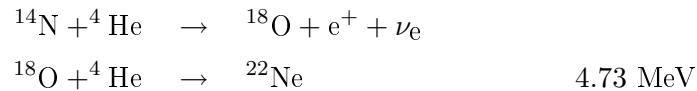
Reaction (2) is favoured by the existence of a resonance at 287 keV, which results in a  ${}^{12}\text{C}$  nucleus excited 7.65 MeV above the ground state.<sup>9</sup> The lifetime of this excited state is very small (about  $5 \times 10^{-17}$  s!), and normally decays straight back to  ${}^4\text{He} + {}^8\text{Be}$ , but 1 in  $\sim 2400$  decays is to a ground-state  ${}^{12}\text{C}$  nucleus, with the emission of two photons. These decays are irreversible, and so a population of  ${}^{12}\text{C}$  nuclei slowly builds up.

### 13.6.2 Further helium-burning stages

Once carbon has been created, still heavier nuclei can be built up:



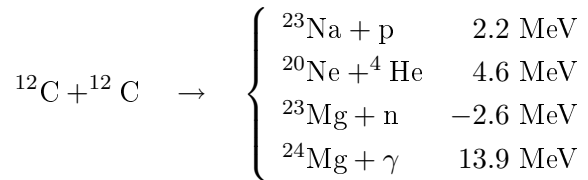
These processes therefore generate C, O, and Ne.  ${}^{12}\text{C}$  and  ${}^{16}\text{O}$  are the most abundant nuclei at the end of He burning (and the most cosmically abundant elements after H and He, with about 1 C or O for every  $10^3$  hydrogens, or every 100 heliums) The situation is more complicated for  ${}^{14}\text{N}$ , which is enhanced during CNO processing<sup>10</sup> but which is destroyed during He burning by the reactions



## 13.7 Advanced burning

### 13.7.1 Carbon burning

After exhaustion of  ${}^4\text{He}$ , the core of a high-mass star contracts further, and at  $T \sim 10^8\text{--}10^9\text{K}$  *carbon burning* can take place:




---

<sup>9</sup>Hoyle (1954) deduced that such a resonance in a previously unknown excited state of carbon must exist to allow an  $\alpha$  particle to combine with an  ${}^8\text{Be}$  with sufficient probability for the triple-alpha process to proceed.

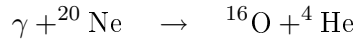
<sup>10</sup>All the initial  ${}^{12}\text{C}$  and  ${}^{16}\text{O}$  ends up as  ${}^{14}\text{N}$ .

with a temperature dependence of

$$\varepsilon_C \simeq \varepsilon_0 \rho T^{32}$$

### 13.7.2 Neon burning

Neon burning takes place after carbon burning if the core temperature reaches  $\sim 10^9\text{K}$ , but at these temperatures photodisintegration also occurs:

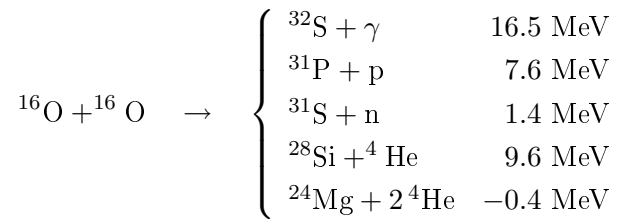


These ‘new’ alpha particles can then react with undissociated neons:



### 13.7.3 Oxygen burning

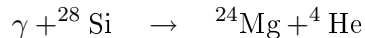
After neon burning the core consists mainly of  ${}^{16}\text{O}$  and  ${}^{24}\text{Mg}$ . Oxygen burning occurs at  $\sim 2 \times 10^9\text{K}$ :



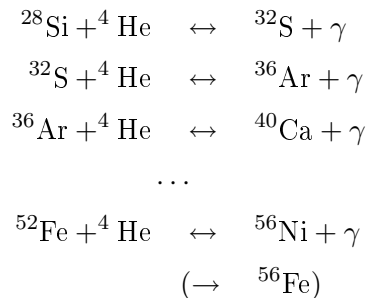
with silicon being the most important product.

### 13.7.4 Silicon burning

At  $\sim 3 \times 10^9\text{K}$ , silicon burning can occur; the Si is slowly photodisintegrated, releasing protons, neutrons, and alpha particles (a process sometimes called ‘silicon melting’ as opposed to ‘silicon burning’). Of particular interest is the reaction



These alpha particles then combine with undissociated nuclei to build more massive nuclei; for example, by way of illustration,

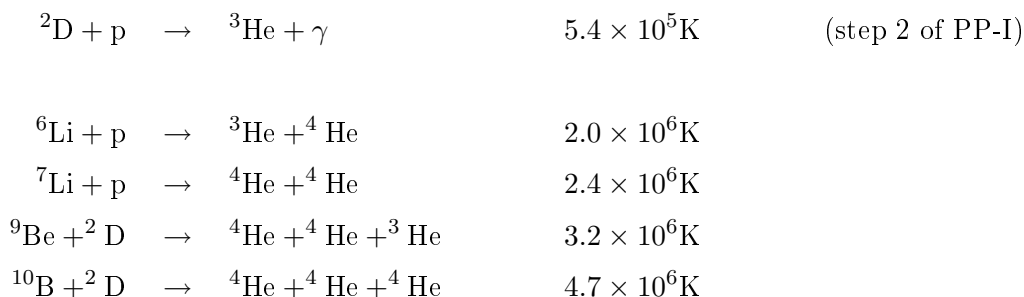


The overall timescale is set by the slowest step, which is the initial photodisintegration of Si.

Because the binding energy per nucleon peaks around mass  $A = 56$  (the ‘iron-peak’ elements Cr, Mn, Fe, Co, Ni) energy is *absorbed* to form heavier nuclei. Elements beyond the iron peak are therefore not formed during silicon burning.

## 13.8 Pre-main-sequence burning

Although not as important as energy-generating sources, some reactions involving light nuclei can occur at  $\sim 10^6\text{K}$  – i.e., lower temperatures than those discussed so far:



These reactions generally *destroy* light elements such as lithium (produced, e.g., primordially) at relatively low temperatures.

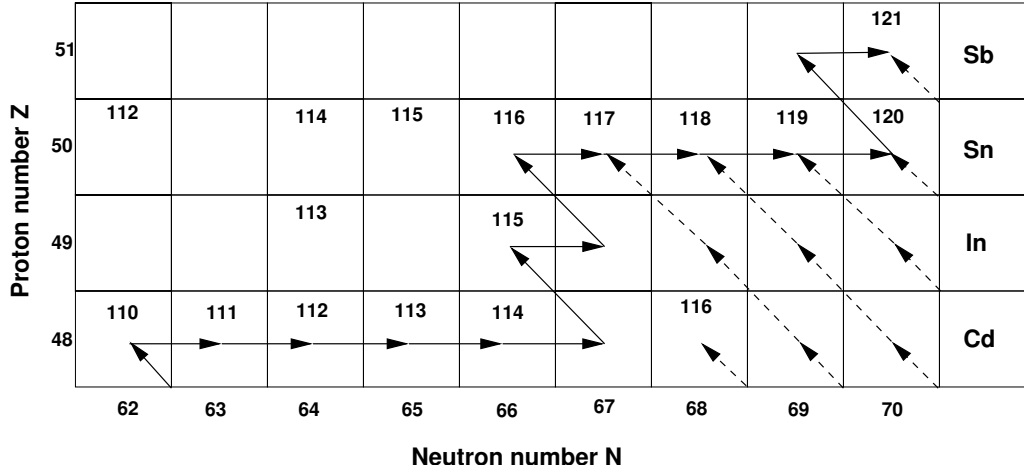
Note that the first step, burning of *pre-existing* deuterium, defines brown dwarfs – objects with cores too cool to produce deuterium by proton-proton reactions.

## 13.9 Synthesis of heavy elements

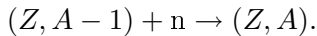
### 13.9.1 Neutron capture: *r* and *s* processes

Carbon burning, oxygen burning etc. can generate heavy elements in the cores of very massive stars, but only as far as the iron peak. However, a quite different set of reactions can occur at lower temperatures ( $\sim 10^8\text{K}$ , comparable to that need for  $3\alpha$  burning).

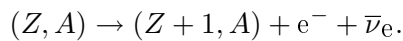
Since neutrons are electrically neutral, they see no Coulomb barrier, and can be absorbed into nuclei even at quite low energies (in fact, heavy nuclei have relatively large neutron-capture cross-sections). Neutron absorption produces a heavier isotope (increases  $A$  but not  $Z$ ); a change in element may then result if the nucleus is unstable to  $\beta$  decay ( $n \rightarrow p + e^- + \bar{\nu}_e$ ).



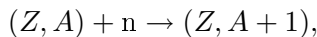
Following the pioneering work of Burbidge, Burbidge, Fowler & Hoyle (Rev. Mod. Phys., 29, 547, 1955), it is conventional to distinguish between *r* and *s* processes, depending on whether neutron capture is *r*apid or *s*low compared to the  $\beta$ -decay timescale. If it is rapid, then more and more massive isotopes accumulate; if it is slow, then decay to a higher- $Z$  element takes place. Suppose we start off with a neutron capture to produce some new isotope:



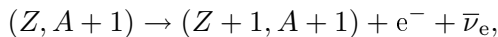
Then if neutron capture happens slowly compared to decay for this new isotope,  $\beta$  decay precedes any further neutron capture, and a new element is formed:



However, if neutron capture is *r*apid then a further isotope is produced,



which will in turn  $\beta$ -decay,



or assimilate a further neutron.

The timescales involved for the *r* and *s* processes are largely set by the relevant nuclear timescales.<sup>11</sup> The *s* process occurs during non-catastrophic evolutionary phases (principally the AGB phase); we *know* this from the observation that technetium occurs in S-type stars (moderately carbon rich M stars). Even the longest-lived technetium isotope, <sup>99</sup>Tc, has a

<sup>11</sup>Just to have some sense of the numbers, the *s* process typically operates on timescales of  $\sim 10^4$  yr at neutron densities of  $\sim 10^{11} \text{ m}^{-3}$ ; corresponding numbers for the *r* process are a few seconds at  $\sim 10^{25} \text{ m}^{-3}$ .

half-life only of order  $10^4$  yr, and so it must be produced within stars during normal evolutionary processes.

Where do the free neutrons come from? For the  $s$  process, the CNO cycle establishes an appreciable abundance of  $^{13}\text{C}$  (step 2 in the sequence set out in Section 13.5), which can react with  $^4\text{He}$ :



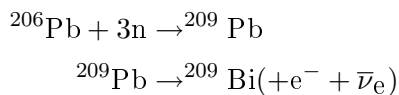
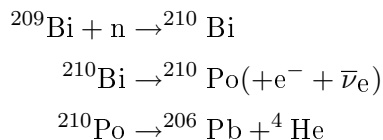
This is the main source of neutrons in AGB stars; at higher temperatures,



is significant.

Neutron-capture cross-sections are exceptionally small for certain nuclear neutron numbers. Because it's harder for the corresponding isotopes to increase in mass through neutron capture, they build up in abundance. We see this effect as peaks in the element-abundance distribution for elements such as  $^{88}_{38}\text{Sr}$ ,  $^{138}_{56}\text{Ba}$ , and  $^{208}_{82}\text{Pb}$ .

Elements beyond bismuth ( $Z = 83$ ) cannot be produced through the  $s$  process, the terminating cycle being



(involving  $Z = 84$  polonium and  $Z = 82$  lead in addition to bismuth).

Many, but not all, elements at lower atomic masses can be produced by both  $r$  and  $s$  processes;  $s$ -only products include  $^{87}_{38}\text{Sr}$  and  $^{187}_{76}\text{Os}$ .

The  $r$  process requires very high neutron fluxes, so that neutron capture rates exceed or compete with  $\beta$ -decay rates. These conditions can only occur during catastrophic, short-timescale phases – supernova explosions. Although some isotopes can be produced by both processes, in general there are significant differences between their products.

	115	116	117	118	119	120	121	122	123	124	125	126	127	128
$_{83}\text{Bi}$									$\epsilon$	$\epsilon$	$\epsilon$	100	$\beta$	$\alpha$
$_{82}\text{Pb}$					$\epsilon$	$\epsilon$	$\epsilon$	1.42	$\epsilon$	24.1	22.1	52.3	$\beta$	$\beta$
$_{81}\text{Tl}$					$\epsilon$	$\epsilon$	$\epsilon$	29.5	$\beta$	70.5	$\beta$	$\beta$		
$_{80}\text{Hg}$	$\epsilon$	0.15	$\epsilon$	10.0	16.8	23.1	13.3	29.8	$\beta$	6.9	$\beta$			
$_{79}\text{Au}$	$\epsilon$	$\epsilon$	$\epsilon$	100	$\beta$	$\beta$								

Figure 13.4: Isotopes of gold–bismuth. The top row lists the number of neutrons in the isotope, while the atomic number (number of protons) is given by the element name. Unstable isotopes decay by conversion of a proton to a neutron (electron capture,  $\epsilon$ ), conversion of a neutron to a proton ( $\beta$  decay), or emission of a helium nucleus ( $\alpha$  decay,  $\text{Bi}^{211}$  only). Numbers give natural percentage abundances of stable isotopes (blanks are for isotopes that do not occur in nature).

The dashed line shows the  $s$ -process path from the only stable isotope of gold ( $\text{Au}^{197}$ ) to the only stable isotope of bismuth ( $\text{Bi}^{209}$ ).  $\text{Hg}^{204}$  is an example of an isotope that can be made only by the  $r$  process.

### 13.9.2 The $p$ process (for reference only)

In their seminal paper, Burbidge, Burbidge, Fowler & Hoyle ( $\text{B}^2\text{FH}$ ) identified the need for a process to create certain relatively proton-rich nuclei, heavier than iron, that cannot be produced by either of the  $r$  or  $s$  processes (e.g.,  $^{190}\text{Pt}$ ,  $^{168}\text{Yb}$ ).

They originally envisaged a proton-capture process, but we now believe that these proton-rich nuclei are not produced by addition of protons, but by removal of neutrons by photodisintegration (i.e., impact by high-energy photons).<sup>12</sup> This occurs through neutron photodisintegration (ejection of a neutron) or  $\alpha$  photodisintegration (emission of an  $\alpha$  particle). These processes require high temperatures (i.e., high-energy photons), and is believed to occur during core collapse of supernovae.

## 13.10 Summary

Hydrogen and helium were produced primordially. After these, CNO are the most abundant elements, with CO produced through helium burning,<sup>13</sup> with nitrogen generated in CNO processing.

Stars more massive than  $\sim 8M_{\odot}$  go on to produce elements such as neon, sodium, and magnesium, with stars more massive than  $\sim 11M_{\odot}$  proceeding to silicon burning, thereby generating nuclei all the way up to the iron peak.

<sup>12</sup>Luckily, ‘photodisintegration’ fits the description ‘ $p$  process’ as well as ‘proton capture’ does! There *is* a proton-capture mechanism, now called the  $rp$  process, but it is generally less important than the  $p$  process.

<sup>13</sup>The balance between C and O is determined by the balance between the rate of production of C and the rate of destruction (in O formation). If the ratio favoured O only a little more, then we wouldn’t be here.

Subsequent processing primarily involves neutron capture (although other processes, such as spallation and proton capture, have a small role).

The timescales for various burning stages are progressively shorter, as energy production rates increase to compensate increasing energy losses (e.g., by increasing neutrino losses). Only massive stars have enough gravitational potential energy to power the most advanced burning stages, so we review the timescales for a 25- $M_{\odot}$  star:

Burning stage	Timescale	$T_c/10^9\text{K}$	$\rho_c$ (kg m <sup>-3</sup> )	Products
H	$7 \times 10^6$ yr	0.06	$5 \times 10^4$	He; N (CNO process)
He	$5 \times 10^5$ yr	0.1	$7 \times 10^5$	C, O
C	$6 \times 10^2$ yr	0.6	$2 \times 10^8$	Ne, Na, Mg, etc.
Ne	$1 \times 10^0$ yr	1	$4 \times 10^9$	O, Na, Mg, etc.
O	$5 \times 10^{-1}$ yr	2	$1 \times 10^{10}$	Si, S, P, etc.
Si	1 d	3	$3 \times 10^{10}$	Mn, Cr, Fe, Co, Ni etc.



## Section 14

# Supernovae

### 14.1 Observational characteristics

Supernovae (SNe) are classified principally on the basis of their spectral morphology at maximum light:

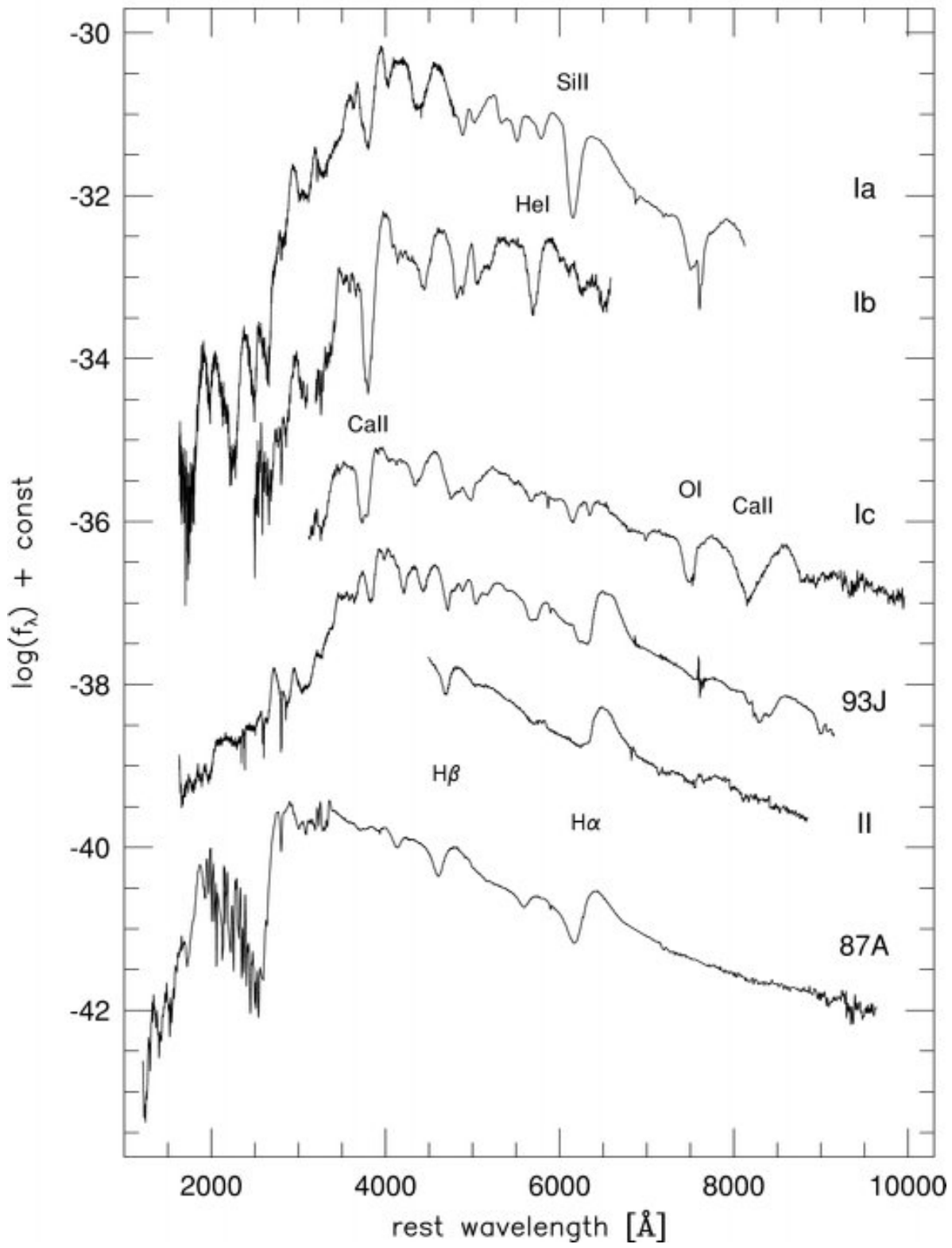
Hydrogen present?	No:	Type I
		Silicon? Yes: Ia
		No: Helium? Yes: Ib
		No: Ic
	Yes:	Type II (II-L, II-P, IIn, Peculiar)

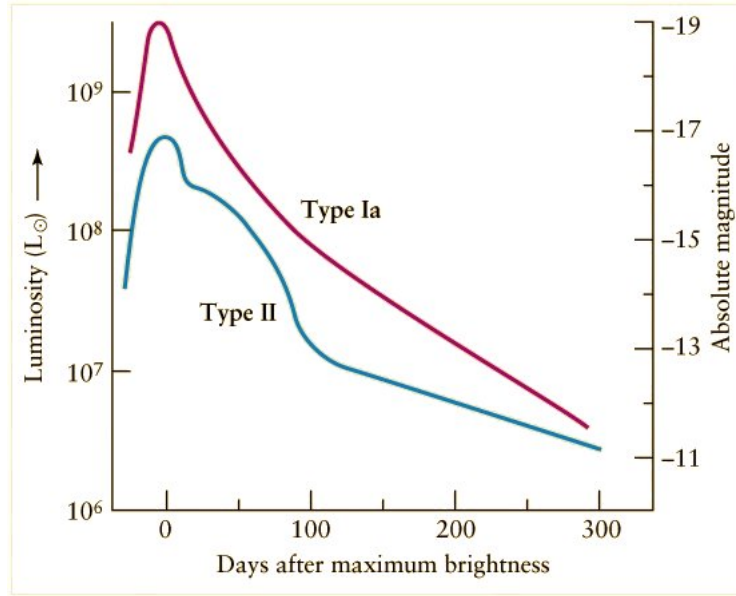
[Our discussion of nucleosynthesis should now inform this empirical classification: e.g., abundant silicon can only result from exposure of material that has undergone advanced burning stages.]

Type II is subclassified according to light-curve morphology; II-L shows a *Linear* decrease in magnitude with time, while II-P supernovae show a *Plateau*. While type II SNe generally show broad lines (corresponding to ejection velocities of thousands of  $\text{km s}^{-1}$ ), some show relatively *narrow* lines (few hundred  $\text{km s}^{-1}$ ); these are classified IIn.

Note that the classification originated in low-resolution photographic spectra, and in the light of modern data is seen to be fairly rough; some spectra are intermediate between these types, and some supernovae may appear as different types at different times. As we shall see, the most important *physical* difference is between Type Ia SNe and ‘the rest’ (that is, between ‘thermonuclear’ & ‘core-collapse supernovae’) – and we will begin with ‘the rest’.

Spectra of SN at maximum





## 14.2 Types Ib, Ic, II

These subtypes collectively constitute the ‘core collapse supernovae’. They occur almost exclusively in the arms of spiral galaxies – strong circumstantial evidence that they are the end points of evolution of short-lived massive stars.

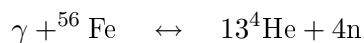
### 14.2.1 The death of a massive star

Although the composition of the outer layers of a star may influence the spectral appearance of its supernova explosion, the key physical processes take place in the stellar core.

As sequential burning processes exhaust their respective fuels in the core, it contracts, generating internal energy. In ‘normal’ evolutionary stages, this leads to the activation of the next fusion process; thermal energy increases and further contraction is opposed.

However, in the final evolutionary stages, the opposite happens; energy is *extracted*, pressure support is further removed, and gravitational contraction becomes gravitational collapse. There are two significant energy-extraction processes relevant to late-stage stellar evolution: photodisintegration, and inverse beta decay.

- (i) The contracting core eventually reaches temperatures sufficient to photodisintegrate iron nuclei (the helium-iron phase transition;  $T \sim 10^9\text{K}$ ):

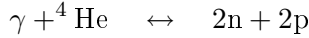


The disintegration requires the same energy as released in building the iron from helium in the first place,

$$Q = [13m(^4\text{He}) + 4m(\text{n}) - m(^{56}\text{Fe})]c^2 = 124.4 \text{ MeV}$$

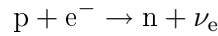
or  $2 \times 10^{14} \text{ J kg}^{-1}$ . About  $3/4$  of the iron is dissociated in this way if the core reaches  $\rho \simeq 10^{12} \text{ kg m}^{-3}$ ,  $T \simeq 10^{10}\text{K}$ .

Endothermic photodissociation of  $^4\text{He}$  can also occur at somewhat higher temperatures:



$$(5 \times 10^{14} \text{ J kg}^{-1}).$$

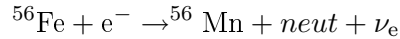
(ii) Electron capture by inverse  $\beta$  decay may also occur; schematically,



although in practice the protons are bound in nuclei:

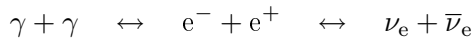


e.g.,



This neutronization occurs at high densities ( $\rho \simeq 10^{12}\text{--}10^{13} \text{ kg m}^{-3}$ ), and produces a copious neutrino flux (as well as a copious neutron flux, which feeds  $r$ -processing).

Neutrinos are also generated by pair production,



Remarkably, it is the neutrinos that carry off  $\sim 90\%$  of the energy released – the radiant and kinetic energies are minor perturbations.

The timescale associated with these processes is the dynamical free-fall timescale,

$$t_{\text{dyn}} = \sqrt{\frac{2r^3}{Gm(r)}} \simeq \sqrt{(G\rho^{-1})} \quad (12.2)$$

which is very short for such high densities – of order 1 ms. The velocities are correspondingly large (up to a quarter the speed of light!). The collapse is therefore indeed catastrophic, and is almost unimpeded until halted by neutron degeneracy; the core briefly achieves a density  $2\text{--}3 \times$

that of nuclear matter before rebounding to leave a neutron star. The rebound sends a shock wave through the overlying layers of the star, which is infalling on a much longer timescale; the shock reverses the infall resulting in an outwards explosion, which we see as the supernova.

The remnant is normally a neutron star, but just as there is a limit to mass of white dwarfs (supported by electron degeneracy pressure),  $\sim 1.4M_{\odot}$ , so there is a limit to the mass of neutron stars (supported by neutron degeneracy pressure),  $\sim 3M_{\odot}$ . If the remnant mass exceeds this limit, a black hole results.<sup>1</sup>

### 14.2.2 Light-curves

Type II SN are thought to arise from red supergiants (as has now been directly observed in several instances). The spectra of these SNe near maximum show roughly normal abundances (in particular, hydrogen is present), with velocities of  $\sim \pm 5000 \text{ km s}^{-1}$ , because we're seeing material from the near-normal outer layers of the progenitor.

The extended outer structure retains much of the heat deposited by the shock, and the initial light-curve in this case is dominated by release of this energy over several weeks.

Evidently, though, Types Ib and Ic, with their H-poor spectra, have lost most of their outer hydrogen envelopes, most probably as a result of strong stellar winds (or through binary interaction).<sup>2</sup> Type I SN (of all types) therefore originate in more compact structures, and their light-curves require an alternative source of heating – radioactive decay. The light-curve decay timescale in SN 1987A corresponds closely to the timescales for radioactive decay of  $^{56}\text{Co}$  to  $^{56}\text{Fe}$  (half-life 77d).<sup>3</sup>

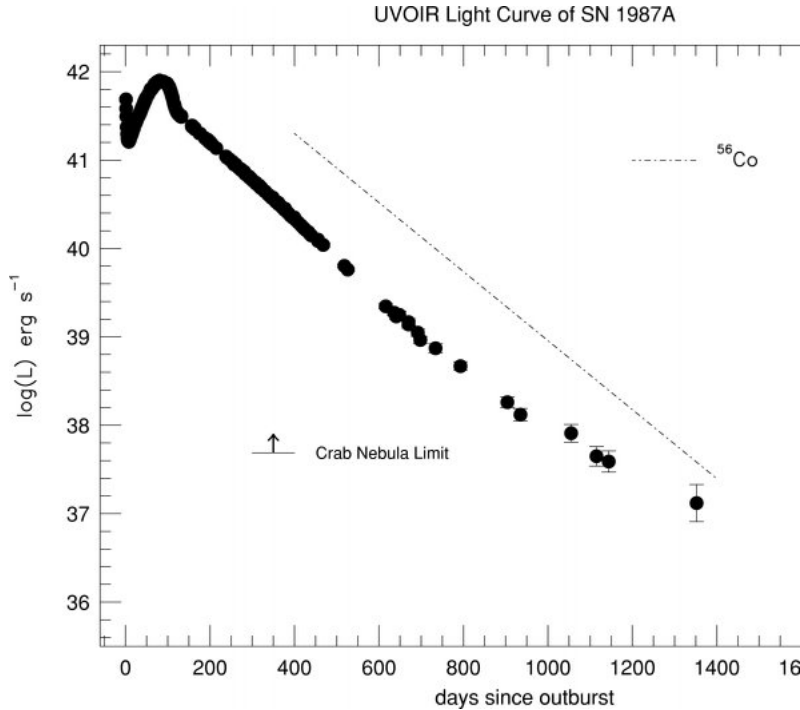
Maximum absolute visual magnitudes of core-collapse supernovae are typically  $-17$  to  $-18$ , with light-curves that are rather diverse, as a result of the differences in the structure of the body surrounding the collapsed core.

---

<sup>1</sup>Degenerate matter has sufficient density that the dominant contribution to the pressure results from the Pauli exclusion principle, arising because the constituent particles (fermions) are forbidden from occupying identical quantum states. Any attempt to force them close enough together that they are not clearly separated by position must place them in different energy levels. Therefore, reducing the volume requires forcing many of the particles into higher-energy quantum states. This requires additional compression force, and so is felt as a resisting pressure. The relevant fermions result in electron or neutron degeneracy pressure.

<sup>2</sup>Short gamma-ray bursts are generally believed to be associated with the collapse of Wolf-Rayet stars.

<sup>3</sup>The  $^{56}\text{Co}$  is in turn produced from the faster (6.1-d) decay of  $^{56}\text{Ni}$ . The late-time fading of 1987A, more than  $\sim 3$  yr after maximum, appears to correspond to decay of  $^{57}\text{Co}$ .



## 14.3 Type Ia SNe

### 14.3.1 Observational characteristics

The light-curves can reach  $M(V) \simeq -19$  ( $\sim 10^{10}L_{\odot}$ ) at maximum, the most luminous of the normal supernovae. They typically show a rather rapid initial decline (for  $\sim 30$ d after maximum), followed by an exponential decay (i.e., linear in magnitude),

$$L = L_0 \exp \{-t/\tau(\text{Ia})\}$$

with  $\tau(\text{Ia}) \simeq 77$ d (the  $^{56}\text{Co}$  decay timescale).

Velocities of up to  $20,000 \text{ km s}^{-1}$  are seen in the absorption- and emission-line spectra, with lines due to elements such as magnesium, silicon, sulfur, and calcium near maximum light.

Type Ia SNe occur in both spiral and, uniquely, elliptical galaxies. Because elliptical galaxies contain no massive stars, Ia SNe can't be core-collapse objects (see Section 14.2.1).

### 14.3.2 Interpretation

Type Ia SNe are believed to be the result of mass transfer onto a white dwarf (WD) in a binary system (or possibly through WD-WD mergers). Eventually the WD is pushed over the Chandrasekhar mass limit ( $1.4M_{\odot}$ ), electron degeneracy is overcome, and the object starts to

collapse; the conversion of gravitational energy to thermal energy drives the temperature to values where carbon burning can occur. The temperature increases, carbon burning accelerates – and a thermonuclear runaway occurs, throughout the star (generating the silicon observed in the spectrum).

Since these processes occur under essentially the same conditions irrespective of evolutionary history, all type Ia SNe are expected to be closely similar – a crucial aspect of their use as ‘standard candles’ in cosmological applications, where they are the only objects sufficiently luminous, and sufficiently ‘standard’, to be useful at large distances.

This standardization is observed to be the case in practice, although there are some systematic differences from object to object; e.g., some are a bit brighter than others, and the brighter events have slightly slower fades from maximum. This evidently relates to the details of the SN event – i.e., how the thermonuclear runaway progresses.

Two distinct routes have been identified for fusion processes to propagate. One is subsonic burning, or ‘deflagration’; the other is supersonic ‘detonation’. Current models suggest that carbon burning starts as a subsonic deflagration and moves to supersonic detonation; slightly different timescales for this process yield slightly different observational characteristics. The energy of the explosion is enough to disrupt completely the original object.

## 14.4 Pair-instability supernovae (for reference only)

If *extremely* massive stars exist ( $\gtrsim 130M_{\odot}$ ) core temperatures may become so great, before the fusion cascade is complete, that high-energy photons ( $\gamma$  rays) in the core annihilate, creating matter-antimatter pairs (mostly  $e^{-}/e^{+}$ ).

Once pair production starts to become the dominant mechanism for  $\gamma$ -ray capture, these photons’ mean free path starts to decrease; this leads to an increase in core temperature, further increasing the photon energy, in turn further decreasing the mean free path. This leads to a runaway instability, removing photons; and as the pressure support provided by the radiation is removed, outer layers fall inward, resulting in what is predicted to be an exceptionally bright supernova explosion.

In such a pair instability supernova (PISN), the creation and annihilation of positron/electron pairs causes the core to be so unstable that it cannot gravitationally collapse further; *everything* is ejected, leaving no remnant.

Stars which are rotating fast enough, or which do not have low metallicities, probably do not collapse in pair-instability supernovae due to other effects (e.g., the mass of high-metallicity stars is constrained by the Eddington limit).

No pair-production supernova has been identified with certainty, but the brightest supernova on record, SN 2006gy (in NGC 1260), is the best candidate. Studies indicate that perhaps  $\sim 40M_{\odot}$  of  $^{56}\text{Ni}$  were released – almost the entire mass of the star’s core regions.  $^{56}\text{Ni}$  decays to  $^{56}\text{Co}$  with a half-life of 6.1 d; in turn the cobalt decays with a half-life of 77 days.